World Academy of Science, Engineering and Technology
International Journal of Mechanical and Mechatronics Engineering
Vol:5, No:1, 2011

Simulation of Heat Transfer in the Multi-Layer Door of the Furnace

U. Prasopchingchana

Abstract—The temperature distribution and the heat transfer rates through a multi-layer door of a furnace were investigated. The inside of the door was in contact with hot air and the other side of the door was in contact with room air. Radiation heat transfer from the walls of the furnace to the door and the door to the surrounding area was included in the problem. This work is a two dimensional steady state problem. The Churchill and Chu correlation was used to find local convection heat transfer coefficients at the surfaces of the furnace door. The thermophysical properties of air were the functions of the temperatures. Polynomial curve fitting for the fluid properties were carried out. Finite difference method was used to discretize for conduction heat transfer within the furnace door. The Gauss-Seidel Iteration was employed to compute the temperature distribution in the door.

The temperature distribution in the horizontal mid plane of the furnace door in a two dimensional problem agrees with the one dimensional problem. The local convection heat transfer coefficients at the inside and outside surfaces of the furnace door are exhibited.

***Keywords*—**Conduction, heat transfer, multi-layer door, natural convection

I. Introduction

HEAT loss from a multi-layer door of a furnace is a combination problem of multi-layer conduction, natural convection and radiation. At present, several research works [1-11] have been devoted to investigate the conduction, natural convection and radiation phenomena. Prasopchingchana and Laipradit [1] performed a simulation of heat transfer in the glass panel of an oven using an empirical correlation for natural convection heat transfer on the surface of the glass panel. Bilgen [2] carried out a numerical and experiment study of conjugate heat transfer by conduction and natural convection on a heated vertical wall. Simulation of natural convection and radiation in the gas cavity and heat conduction in the walls of an enclosure was performed by Kuznetsov and Sheremet [3]. Nouanegue and Bilgen [4] carried out a numerical study on vertical channel solar chimneys with a practical geometry, which consist of two dimensional channel boarded by two solid walls. Xaman et al. [5] study laminar and turbulent natural convection combined with surface thermal radiation in a square cavity with a glass wall. Zrikem et al. [6] numerically investigated coupled heat transfers by conduction, natural convection and radiation in hollow structures heated from below or above. Oztop and co-workers [7] examined the combined conduction and mixed convection flow field and temperature distribution in an enclosure in the presence of vertical partition with finite thickness and thermal conductivity. Nouanegue et al. [8] investigated conjugate heat transfer by natural convection, conduction and radiation in open cavities in which a uniform heat flux is applied to the inside surface of the solid wall facing the opening. Chiu and Yan [9] carried out a numerical study in the radiation effect on the characteristics of the mixed convection fluid flow and heat transfer in inclined ducts. The effect of conduction of horizontal walls on natural convection heat transfer in a square cavity is numerically investigated by Mobedi [10]. Molla and Hossain [11] examined the effect of thermal radiation on a study two-dimensional mixed convection laminar flow of viscous incompressible optically thick fluid along a vertical wavy surface.

This research aims to study the coupling between multi-layer conduction, natural convection and surface radiation on the multi-layer door of the furnace. The work used the Churchill and Chu [12] empirical correlation in the simulation to compute the average convection heat transfer coefficients. Later, the local convection heat transfer coefficients were determined. Then, radiation heat transfer coefficients were computed. Finally, the temperature distribution and total heat loss from the inside of the furnace to room air through the multi-layer door of the furnace were investigated.

II. Model gometry

This research has been treated as a two dimensional steady-state problem. There was hot air on the inside surface of the multi-layer door and room air on the outside surface of the multi-layer door.

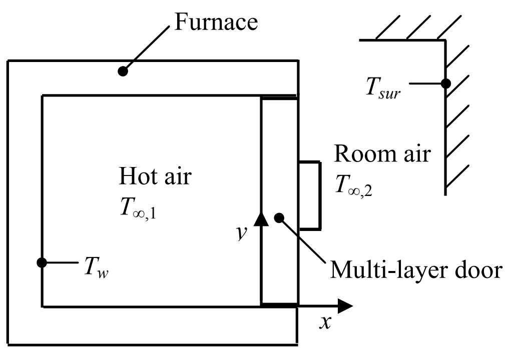

Fig. 1 Model geometry

The top and bottom sides of the multi-layer door were assumed to be insulated. The multi-layer door of the furnace is 50 cm. wide, 50 cm. high and 20.3 cm. thick. The multi-layer

U. Prasopchingchana is with the Mechanical Engineering Department, Burapha University, Chonburi 20131 THAILAND (phone: 66-3810-2222 Ext. 3385 Ext. 104; fax: 66-3874-5806; e-mail: uthai@buu.ac.th).

door of the furnace consists of 3 layers: fire clay brick, glass fiber insulation and steel sheet. The thermal conductivity values [13] and the thickness values of each layer are shown in Table 1.

TABLE I
PROPERTIES OF THE MULTI-LAYER DOOR

Layer	Material	Thickness (m)	Thermal conductivity (W/m·K)
1	Fire clay brick	0.1	1.09
2	Glass fiber insulation	0.1	0.038
3	Steel sheet	0.003	28

The emissivity values [13] at the surfaces of the multi-layer door inside and outside of the furnace are 0.75 and 0.066 respectively. The temperatures at the furnace wall surfaces equaled the hot air temperatures in the cavity. Also, the temperatures of the surrounding area equaled the room air temperatures.

III. MATHEMATICAL MODELS

Newton's law of cooling was employed to determine the heat transfer rates at the surfaces of the furnace door. To determine the average Nusselt number, the work used the Churchill and Chu empirical correlation [12]:

$$\overline{Nu}_y = \left\{ 0.825 + \frac{0.387 Ra_y^{1/6}}{\left[1 + (0.492/Pr)^{9/16}\right]^{8/27}} \right\}^2 \tag{1}$$

where Ra_y is the Rayleigh number and Pr is the Prandtl number at the film temperatures. The film temperatures are

$$T_f = \left((T_s)_{ave} + T_\infty\right)/2 \tag{2}$$

where $(T_s)_{ave}$ is the average temperature at the door surfaces and T_∞ is the ambient temperature. The average convection heat transfer coefficients were obtained from

$$\bar{h}_y = \overline{Nu}_y \frac{k_f}{y} \tag{3}$$

where k_f is thermal conductivity of air. The local convection heat transfer coefficients could be obtained from

$$\bar{h}_{y+\delta y} = \frac{1}{y+\delta y}\left(\int_0^y h_y \delta y + \int_y^{y+\delta y} h_{\delta y} \delta y \right)$$

$$(y+\delta y)\bar{h}_{y+\delta y} = y\left(\frac{1}{y}\int_0^y h_y \delta y \right) + \delta y \left(\frac{1}{\delta y}\int_y^{y+\delta y} h_{\delta y}\delta y \right)$$

$$(y+\delta y)\bar{h}_{y+\delta y} = y\bar{h}_y + \delta y \bar{h}_{\delta y}$$

$$\bar{h}_{\delta y} = \frac{(y+\delta y)\bar{h}_{y+\delta y} - y\bar{h}_y}{\delta y} \tag{4}$$

Newton's law of cooling was used to determine the convection heat transfer rates at the furnace door surfaces. The convection heat transfer rates at the furnace door surfaces are

$$q_{\delta y} = \bar{h}_{\delta y} w \delta y (T_\infty - T_s) \tag{5}$$

where w is the furnace door width.

Radiation heat transfer from the furnace wall surfaces to the inner door surface and from the outer door surface to the surrounding area was included in the problem. The nonlinear equations of radiation heat transfer were linearized. Thus, the radiation heat transfer equations are

$$q_{r,w} = h_{r,1} A\left(T_w - T_{s,1}^{(k)} \right) \tag{6}$$

and

$$q_{r,sur} = h_{r,2} A\left(T_{s,2}^{(k)} - T_{sur} \right) \tag{7}$$

where $h_{r,1}$ is the radiation heat transfer coefficient between the furnace wall surfaces and the furnace door surface, and $h_{r,2}$ is the radiation heat transfer coefficient between the furnace door surface and the surrounding area. The radiation heat transfer coefficients are

$$h_{r,1} = \varepsilon_1 \sigma \left(T_w + T_{s,1}^{(k-1)} \right)\left(T_w^2 + \left[T_{s,1}^{(k-1)} \right]^2 \right) \tag{8}$$

and

$$h_{r,2} = \varepsilon_2 \sigma \left(T_{sur} + T_{s,2}^{(k-1)} \right)\left(T_{sur}^2 + \left[T_{s,2}^{(k-1)} \right]^2 \right) \tag{9}$$

where ε is emissivity and σ is the Stefan-Boltzmann constant.

All properties of hot air and room air around the inside and the outside of the furnace door surfaces were obtained from NIST (National Institute of Standards and Technology) Standard Reference Database 23, Version 7.0 by polynomial curve fitting:

$$x = a_1 + a_2 T_f + a_3 T_f^2 + \ldots + a_n T_f^{n-1} \tag{10}$$

where x are the air properties, a_n are the polynomial curve fitting coefficients and T_f is the film temperature of air. The errors of the properties derived from polynomial curve fitting are less than 0.1 percent. For all properties, n is 10.

The volumetric thermal expansion coefficient is

$$\beta = -\frac{1}{\rho}\left(\frac{\partial \rho}{\partial T} \right)_P$$

$$\beta = -\frac{1}{\rho}\left(a_2 + 2a_3 T_f + 3a_4 T_f^2 + \ldots + (n-1)a_n T_f^{n-2} \right)_P \tag{11}$$

Within the thickness of the furnace door, the heat diffusion equation was used to calculate the temperature distribution:

$$\frac{\partial^2 T}{\partial x^2} + \frac{\partial^2 T}{\partial y^2} = 0 \tag{12}$$

The finite difference method was used to discretize Eq. (12) and it yielded

$$T_{i,j}^{(k)} = \left[\Delta y^2 \left(T_{i+1,j}^{(k-1)} + T_{i-1,j}^{(k)} \right) + \Delta x^2 \left(T_{i,j+1}^{(k-1)} + T_{i,j-1}^{(k)} \right) \right] / 2\left(\Delta y^2 + \Delta x^2 \right) \tag{13}$$

The finite difference equation for the nodes close to the interfaces as shown in Fig. 2 is

$$T_{i,j}^{(k)} = \left(\frac{T_{i-1,j}^{(k)}}{R1} + \frac{T_{i+1,j}^{(k-1)}}{R2} + \frac{T_{i,j-1}^{(k)}}{R3} + \frac{T_{i,j+1}^{(k-1)}}{R3} \right) / \left(\frac{1}{R1} + \frac{1}{R2} + \frac{1}{R3} + \frac{1}{R3} \right) \quad (14)$$

where $R1$, $R2$ and $R3$ are the thermal resistances. The thermal resistances are

$$R1 = \frac{\Delta x_A}{k_A \Delta y w} + \frac{\Delta x_B}{k_B \Delta y w}$$

$$R2 = \frac{\Delta x_B}{k_B \Delta y w}$$

If Δx_A is less than Δx_B, $R3$ is

$$R3 = \frac{\Delta y}{k_B \Delta x w}$$

If Δx_A is more than Δx_B, $R3$ is

$$R3 = \left(\frac{k_A((\Delta x/2) - \Delta x_B)w}{\Delta y} + \frac{k_B(\Delta x_B + (\Delta x/2))w}{\Delta y} \right)^{-1}$$

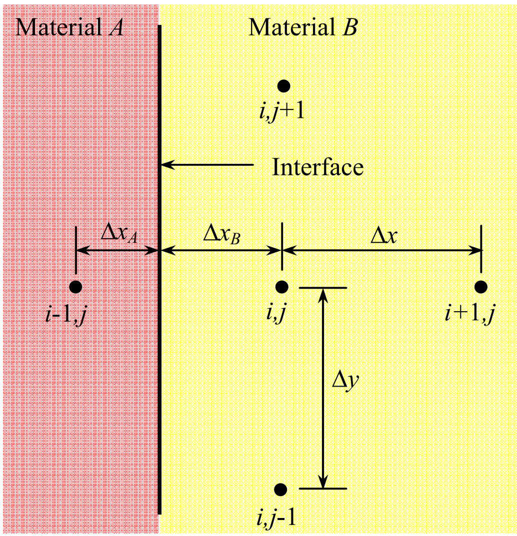

Fig. 2 Nodes close to the interface

The top and bottom sides of the furnace door were assumed to be insulated. The finite difference equations for the top and bottom sides are

$$T_{i,1}^{(k)} = \frac{\Delta y^2 T_{i-1,1}^{(k)} + \Delta y^2 T_{i+1,1}^{(k-1)} + \Delta x^2 T_{i,2}^{(k-1)}}{2(\Delta y^2 + \Delta x^2)} \quad (15)$$

and

$$T_{i,jm}^{(k)} = \frac{\Delta y^2 T_{i-1,jm}^{(k)} + \Delta y^2 T_{i+1,jm}^{(k-1)} + \Delta x^2 T_{i,jm-1}^{(k)}}{2(\Delta y^2 + \Delta x^2)} \quad (16)$$

At the furnace door surfaces, there are three modes of heat transfer: conduction, convection and radiation. The finite difference equations are

$$T_{1,j}^{(k)} = \left[\frac{k\Delta x}{2\Delta y} T_{1,J-1}^{(k)} + \frac{k\Delta x}{2\Delta y} T_{1,J+1}^{(k-1)} + \frac{k\Delta y}{\Delta x} T_{2,J}^{(k-1)} + (h_1)_j \Delta y T_{\infty,1} + (h_{r,1})_j \Delta y T_w \right] / \left[\frac{k\Delta x}{\Delta y} + \frac{k\Delta y}{\Delta x} + (h_1)_j \Delta y + (h_{r,1})_j \Delta y \right] \quad (17)$$

and

$$T_{im,j}^{(k)} = \left[\frac{k\Delta x}{2\Delta y} T_{im,J-1}^{(k)} + \frac{k\Delta x}{2\Delta y} T_{im,J+1}^{(k-1)} + \frac{k\Delta y}{\Delta x} T_{im-1,J}^{(k)} + (h_2)_j \Delta y T_{\infty,2} + (h_{r,2})_j \Delta y T_{sur} \right] / \left[\frac{k\Delta x}{\Delta y} + \frac{k\Delta y}{\Delta x} + (h_2)_j \Delta y + (h_{r,2})_j \Delta y \right] \quad (18)$$

The finite difference equations for the four corners of the furnace door are

$$T_{1,1}^{(k)} = \left[\frac{k\Delta x}{2\Delta y} T_{1,2}^{(k-1)} + \frac{k\Delta y}{\Delta x} T_{2,1}^{(k-1)} + (h_1)_j \Delta y T_{\infty,1} + (h_{r,1})_j \Delta y T_w \right] / \left[\frac{k\Delta x}{\Delta y} + \frac{k\Delta y}{\Delta x} + (h_1)_j \Delta y + (h_{r,1})_j \Delta y \right] \quad (19)$$

$$T_{1,jm}^{(k)} = \left[\frac{k\Delta x}{2\Delta y} T_{1,jm-1}^{(k)} + \frac{k\Delta y}{\Delta x} T_{2,jm}^{(k-1)} + (h_1)_j \Delta y T_{\infty,1} + (h_{r,1})_j \Delta y T_w \right] / \left[\frac{k\Delta x}{\Delta y} + \frac{k\Delta y}{\Delta x} + (h_1)_j \Delta y + (h_{r,1})_j \Delta y \right] \quad (20)$$

$$T_{im,1}^{(k)} = \left[\frac{k\Delta x}{\Delta y} T_{im,2}^{(k-1)} + \frac{k\Delta y}{\Delta x} T_{im-1,1}^{(k)} + (h_2)_j \Delta y T_{\infty,2} + (h_{r,2})_j \Delta y T_{sur} \right] / \left[\frac{k\Delta x}{\Delta y} + \frac{k\Delta y}{\Delta x} + (h_2)_j \Delta y + (h_{r,2})_j \Delta y \right] \quad (21)$$

and

$$T_{im,jm}^{(k)} = \left[\frac{k\Delta x}{\Delta y} T_{im,jm-1}^{(k)} + \frac{k\Delta y}{\Delta x} T_{im-1,jm}^{(k)} + (h_2)_j \Delta y T_{\infty,2} + (h_{r,2})_j \Delta y T_{sur} \right] / \left[\frac{k\Delta x}{\Delta y} + \frac{k\Delta y}{\Delta x} + (h_2)_j \Delta y + (h_{r,2})_j \Delta y \right] \quad (22)$$

The Gauss Seidel Iteration was used to determine the temperature distribution on the furnace door. The iteration was terminated when the errors in the temperatures were less than 0.00001. The errors in the temperatures were obtained from:

$$E = \left| T_{i,j}^{(k)} - T_{i,j}^{(k-1)} \right| \quad (23)$$

The grid independence tests were performed at 69×168, 103×251 and 204×501. The uniform grid size of 69×168 was used. The heat transfer balance at the inside and outside surfaces of the furnace door was carried out as shown in Table 2.

TABLE II
GRID INDEPENDENCE TESTS.

Grid size	Heat transfer rates at the surfaces of the furnace door (W)	
	Inner surface	Outer surface
69×168	84	84
103×251	84	84
204×501	84	84

The assumptions of this research were the following:
1. The problem was a steady-state condition.
2. Heat conduction in the furnace door was a two dimensional problem.
3. The top and bottom surfaces of the furnace door were insulated.
4. The properties of the furnace door were constant.

IV. RESULTS AND SISCUSSIONS

The temperature distribution on the horizontal mid plane of the furnace door at 1000°C internal temperature and 25°C ambient temperature is shown in Fig. 3. The result in the two dimensional problem agrees with the one dimensional problem.

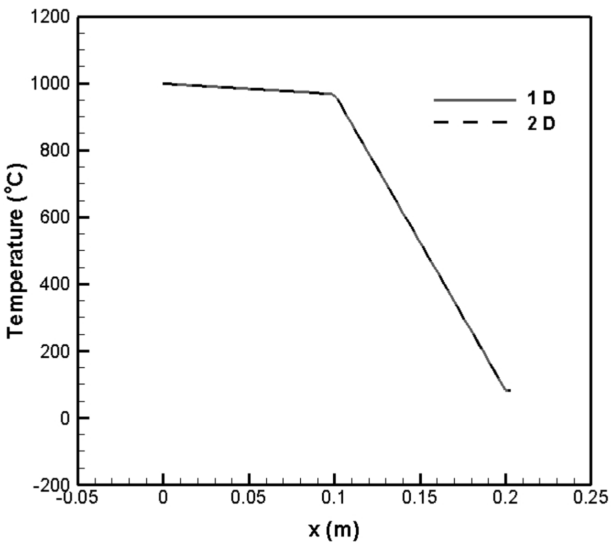

Fig. 3 Temperature distribution on the horizontal mid plane of the furnace door at 1000°C internal temperature and 25°C ambient temperature in one and two dimensional problems.

The heat transfer rates at 20, 25 and 30°C ambient temperature are shown in Fig. 4. The temperatures of the furnace wall surfaces in the x axis vary from 1000°C to 1300°C. The heat transfer rates increase directly with the temperatures of the furnace wall surfaces.

The distribution of the local convection heat transfer coefficients on the surfaces of the furnace door for internal temperature and ambient temperature at 1000 and 25°C, respectively, is shown in Fig. 5. The coefficient values near the top of the furnace door surface inside of the furnace are higher than those in the other regions of the furnace door surface, while the coefficient values of the furnace door surface outside of the furnace are inverse to the furnace door surface inside of the furnace.

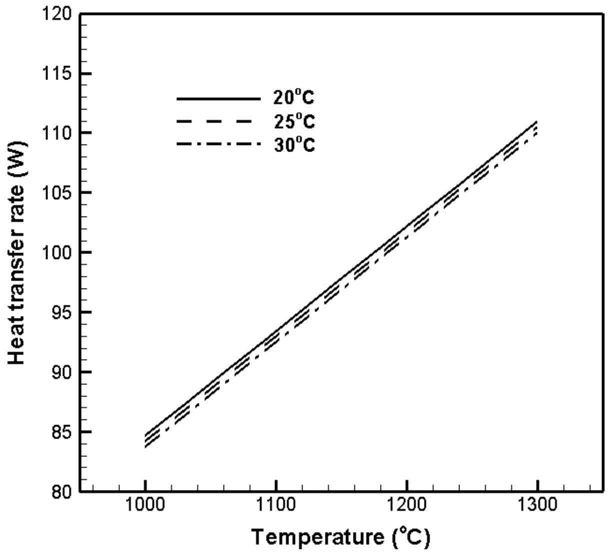

Fig. 4 Heat transfer rates at 20, 25 and 30°C ambient temperature.

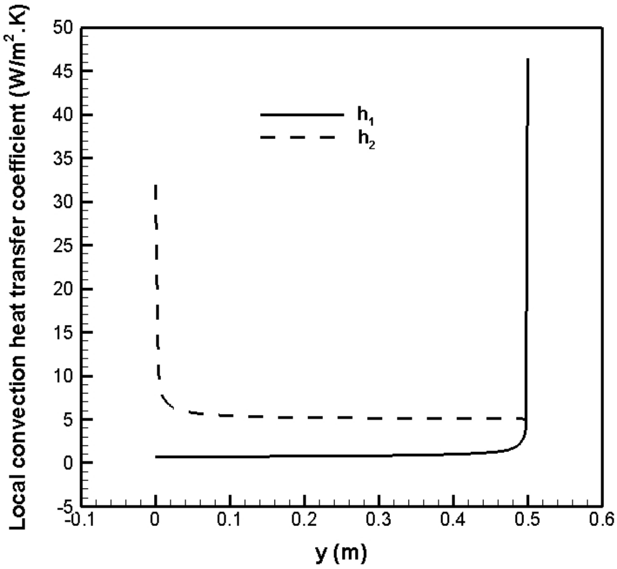

Fig. 5 Local convection heat transfer coefficient distribution on the furnace door surfaces.

The temperature contour in the furnace door at 1000°C internal temperature and 25°C ambient temperature is shown in Fig. 6. The temperature gradients vary with the layers of the furnace door.

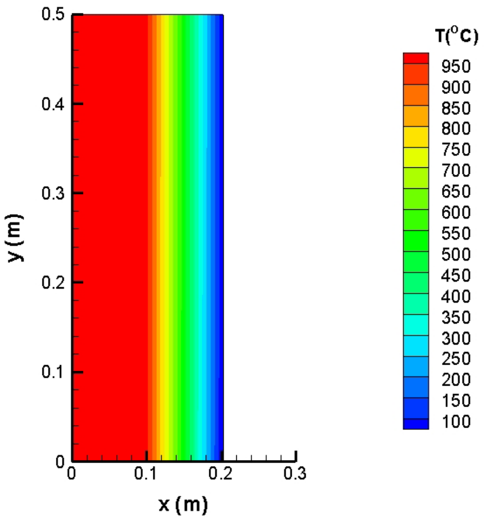

Fig. 6 Temperature contour in the furnace door at 1000°C internal temperature and 25°C ambient temperature.

V. Conclusion

The temperature gradients in the different materials have different values. The temperature distribution in the horizontal mid plane of the two dimensional problem agrees with the result from the one dimensional problem. The highest values of the local heat transfer coefficients occur at the top of the inside surface of the furnace door, and the bottom of the outside surface of the furnace door.

Nomenclature

Symbols

h	Local convection heat transfer coefficient ($W/m^2 \cdot K$)
$\bar{h}$	Average convection heat transfer coefficient ($W/m^2 \cdot K$)
k	Thermal conductivity ($W/m \cdot K$)
$\overline{Nu}$	Average Nusselt number
Pr	Prandtl number
q	Heat transfer rate (W)
Ra	Rayleigh number
T	Temperature (K)
x	Distance in horizontal direction (m)
y	Distance in vertical direction (m)
β	Volumetric thermal expansion coefficient
ρ	Density

Subscripts

ave	Average
f	Fluid
i	Number of nodes in the horizontal direction
im	Maximum number of nodes in the horizontal direction
j	Number of nodes in the vertical direction
jm	Maximum number of nodes in the vertical direction
r	Radiation
s	Surface
sur	Surrounding area
w	Wall surface of the furnace
y	In *y* direction
∞	Ambient
1	Inside the furnace
2	Outside the furnace

Superscript

k	Number of iteration

References

[1] U. Prasopchingchana and P. Laipradit, “Simulation of Heat Transfer in the Glass Panel of an Oven Using an Empirical Correlation for Natural Convection Heat Transfer on the Surfaces of the Glass Panel”, in Proc. the 23rd Conference of Mechanical Engineering Network of Thailand, Chiang Mai, Thailand. 2009.

[2] E. Bilgen, “Conjugate heat transfer by conduction and natural convection”, Applied Thermal Engineering, vol. 29, pp. 334-339. 2009.

[3] G. V. Kuznetsov and M. A. Sheremet, “Conjugate natural convection with radiation in an enclosure”, International Journal of Heat and Mass Transfer, vol. 52, pp. 2215-2223. 2009.

[4] H. F. Nouanegue and E. Bilgen, “Heat transfer by convection, conduction and radiation in solar chimney systems for ventilation of dwellings”, International Journal of Heat and Fluid Flow, vol. 30, pp. 150-157. 2009.

[5] J. Xaman, J. Arce, G. Alvarez and Y. Chavez, “Laminar and turbulent natural convection combined with surface thermal radiation in a square cavity with a glass wall”, International Journal of Thermal Sciences, vol 47, pp. 1630-1638. 2008.

[6] T. Ait-taleb, A. Abdelbaki and Z. Zrikem, Z., “Numerical simulation of coupled heat transfers by conduction, natural convection and radiation in hollow structures heated from below or above”, International Journal of Thermal Sciences, vol. 47, pp. 378-387. 2008.

[7] H. F. Oztop, Z. Zhao and B. Yu, B., “Conduction-combined forced and natural convection in lid-driven enclosures divided by a vertical solid partition”, International Communications in Heat and Mass Transfer, vol. 36, pp. 661-668. 2009.

[8] H. Nouanegue, A. Muftuoglu and E. Bilgen, “Conjugate heat transfer by natural convection, conduction and radiation in open cavities”, International Communications in Heat and Mass Transfer, vol 51, pp. 6054-6062. 2008.

[9] H. C. Chiu and W. M. Yan, “Mixed convection heat transfer in inclined rectangular ducts with radiation effects”, International Journal of Heat and Mass Transfer, vol. 51, pp. 1085-1094. 2008.

[10] M. Mobedi, “Conjugate natural convection in a square cavity with finite thickness horizontal walls”, International Communications in Heat and Mass Transfer, vol. 35, pp. 503-513. 2008.

[11] M. M. Molla and M. A. Hossian, “Radiation effect on mixed convection laminar flow along a vertical wavy surface”, International Journal of Thermal Sciences, vol. 46, pp. 926-935. 2007

[12] S. W. Churchill, and H. H. S. Chu, “Correlating equations for laminar and turbulent free convection from a vertical plate”, International Journal of Heat and Mass Transfer, vol. 18, pp. 1323-1329. 1975.

[13] J. P. Holman, Heat Transfer, 10 ed., McGraw-Hill, New York. 2010.